Desalination and Water Treatment
www.deswater.com
doi: 10.1080/19443994.2013.814381

52 (2014) 4476–4484
June

Taylor & Francis
Taylor & Francis Group

Study on dissolved organic nitrogen (DON) removal by activated carbon adsorption

Li Gu[a,*], Jinli Xu[b], Changlong Ding[a], Xin Yu[b], Huirong Lin[b], Qiang He[a], Jiang Li[a]

[a]*Key laboratory of the Three Gorges Reservoir Region's Eco-environments, Ministry of Education, Institute of Urban Construction and Environmental Engineering, Chongqing University, 174 Shapingba Road, Chongqing 400045, China*
Tel./Fax: 86 23 65126160; email: guli_095@126.com
[b]*Institute of Urban Environment, Chinese Academy of Sciences, 1799 Jimei Road, Xiamen 361021, China*

Received 14 April 2012; Accepted 30 April 2013

ABSTRACT

Dissolved organic nitrogen (DON) is an important issue in drinking water field. This paper deals with DON removal by activated carbon (AC) in batch and fixed bed operation. Adsorption kinetics and equilibrium isotherms in batch operation are investigated while the breakthrough curves in fixed bed operation for DON adsorption at different conditions are obtained. The isotherm results show that the peach carbon is the most suitable type which shows higher adsorption capacity than other ACs. Kinetic data of adsorption are well fitted by the pseudo-second-order kinetic model, and the thermodynamic constants are also evaluated in the study. The results of the fixed bed operation show that, with the increase of the flow rate and the influent concentrations, the breakthrough curve becomes steeper while the break point time decrease. With the increase in the bed height, the breakthrough time increases. Adams-Bohart model is used to describe the initial region of breakthrough curve, while bed depth service time model is applied to predict the breakthrough time for new conditions. Both models give good agreement with experimental curves. This paper reveals the suitable ACs for DON removal and gives the basic data for DON removal in fix bed adsorption.

Keywords: Dissolved organic nitrogen; Activated carbon; Adsorption; Fixed bed

---

1. Introduction

Dissolved organic nitrogen (DON) is the org-N structure of dissolved organic matters [1]. It can react with chlorine or chloramine during disinfection processes and release quantities of toxic disinfection by-products. These nitrogenous disinfection by-products (N-DBPs), including halonitroalkane, nitrosamines, haloacetonitriles, and cyanogens halodes, are recognized to have higher toxicity than the halogen by-products [2]. Hence, it is of great significance and interest in pursuing efficient methods to remove DON.

DON is composed of a series of compounds containing a variety of nitrogen-containing functional groups. It is reported to present a low percentage (about 1.0–5.0% by weight) of NOM (Natural Organic Matters) with a median concentration about 0.30 mg/l in surface water [1]. Algal blooms, water pollution and agricultural nonpoint source pollution can cause

---

*Corresponding author.

a dramatic increase in DON concentration. Higher DON amount commonly present higher risk in N-DBPs formation during disinfection process, though the generation of the given N-DBPs depend on the characteristics of the DON rather than its amount (e.g. hydrophilic fractions in DON played a critical role in DCAcAm (dichloroacetamide) formation than hydrophobic fractions) [3].

Currently, studies about DON are focusing on its structural composition, occurrence, and potential in N-DBPs formation [1,3,4]. Studies about its removal by various techniques can hardly be found. Adsorption, due to its proven efficiency and no harmful byproducts formation, has received great attention in water treatment. As an outstanding adsorbent, activated carbon (AC) is utilized most frequently. The extensive microporous structure, large surface area, and rapid adsorption capability of AC provides effective performances in removing pollutants from water [5–8].

For the adsorption of organic pollutants, previous studies have focused on batch kinetic and equilibrium. For the results of these studies, the ability of AC in removal of some target organic chemicals has been evaluated [9,10]. Though some researchers examined different pretreatment processes including PAC adsorption, $KMnO_4$ oxidation and biochemical oxidation process on DON levels and halogenated N-DBPs formation [11], information about the ability of different ACs in the adsorption of DON is still limited. In addition, in industrial application of the adsorption methods, studies about fixed bed operation are commonly preferred. The behavior and performance of the fixed bed columns need deeply investigation because their results are the basic data for engineering application. As acknowledged, little information is available on the dynamic capacity for DON removal in a continuous flow column.

Purpose of this study is to evaluate the capacities of different ACs in adsorption of DON. The adsorption process is conducted in both batch and fixed bed column system. Equilibrium and kinetic data of the adsorption process are studied to understand the ability of different types of ACs in DON adsorption. Based on the results of fixed bed operation, the effect of the bed depth, initial DON concentrations, and feed flow rates on adsorption breakthrough curve and overall rate coefficient are obtained.

2. Materials and methods

2.1. Chemicals and materials

AC was purchased from National Pharmaceutical Group Chemical Reagent Co., Ltd. (Abbreviated as "NPGC") and Wuxi Chi Kang Activated Carbon Co., Ltd. These AC were crushed and screened and those with particle size of 1–2 mm were selected. Porous properties and surface morphology of these ACs are shown in Fig. 1 and Table 1. Prior to use, these ACs were washed and dried.

DON working solution was prepared using DON stock solution (1.0 g/l), which was prepared by dissolving humic acid (Tianjin Chemical Reagent Co. Ltd., China, purified), tyrosine and arginine into deionized water. The ratio of DOC/DON retained at 10:1.

2.2. Experimental procedure

2.2.1. Adsorption tests carried out in batch system

Adsorption of DON onto ACs was studied firstly in a batch reactor. About 200 ml working solutions with different concentrations were prepared. After addition of different amount of ACs, these flasks were shaken at 298 K. In equilibrium tests, these flasks were shaken for 48 h. Sample was analyzed after 0.45-μm pore-sized membrane filtration.

2.2.2. Continuous adsorption tests

This test was also carried out in a continuous mode by AC used as the fix bed adsorbent. The fixed-bed adsorption unit was a glass column with inside diameter of 1 cm, and length of 15 cm. The solutions with different DON concentrations were pumped into the fixed bed column in constant feeding speed. The solution was withdrawn from the bottom of the column at selected intervals for analysis.

2.2.3. Analysis

DON was quantified by TDN (Total Dissolved Nitrogen) minus NH_4^+–N, NO_3^-–N, and NO_2^-–N ($DON = TDN–NH_4^+–NO_2^-–NO_3^-$) [1]. The TDN concentration was measured by analyzing the NO_3^- concentration by using UV spectrophotometry method after completely digestion, while the other nitrogen compounds were determined according to standard methods [12]. The surface morphology of the carbon was analyzed using a scanning electron microscopy (SEM, JSM-5600LV). Surface area and pore size distributions for the samples were measured using ASAP2020 surface area analyzer using nitrogen adsorption/desorption method. DOC was measured by Shimadzu TOC 4,100 TOC analyzer.

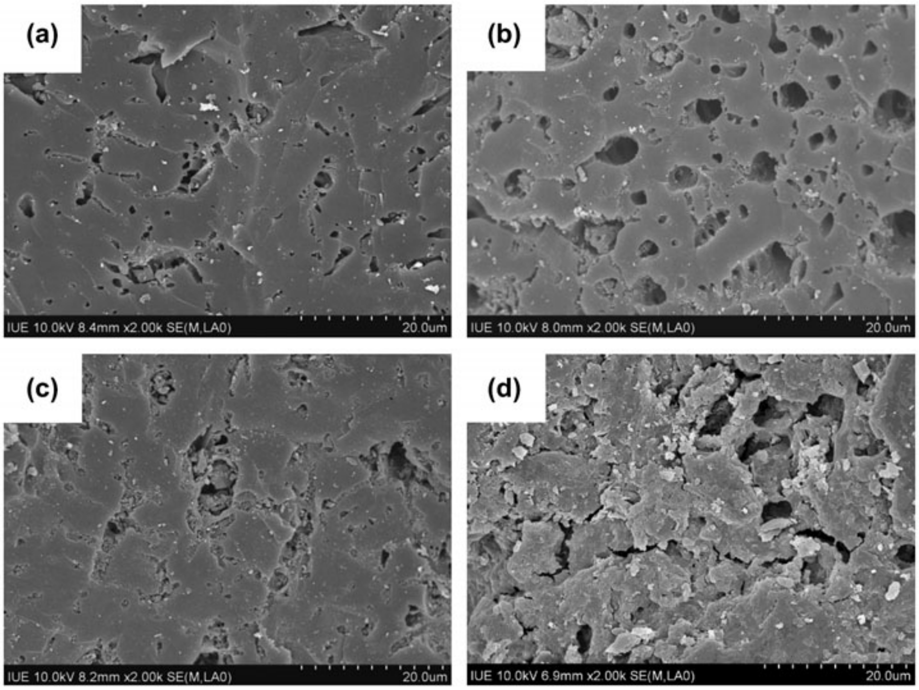

Fig. 1. SEM images of different AC samples (A. TY-8X30 B. TY-202 C. GY-1 D. TY-1.5).

3. Results and discussion

3.1. Adsorption tests carried out in a batch reactor

3.1.1. Adsorption isotherm and capacity

Adsorption isotherm experiments were conducted firstly to probe the capacities of different ACs in DON adsorption in batch reactor. In practice, DON uptake increases gradually with the equilibrium concentration increasing. To make numeric comparison among these carbons, the Freundlich isotherm was applied.

Freundlich equation:

$$q_e = KC_e^{1/n} \tag{1}$$

In Eq. (1), C_e and q_e are the DON concentration (mg/l) and the adsorbed amount (mg/g) of DON at equilibrium [13,14]. The parameter n is the constant of the isotherm model. The equation can be expressed as:

$$\ln q_e = \ln K_f + (1/n) \ln C_e \tag{2}$$

Fig. 2 shows the adsorption isotherm which is interpreted using the Freundlich isotherm model. The estimated model parameters are shown in Table 2.

The fitting process can be seen from Fig. 2. The estimated model parameters in Table 2 provide numeric comparison of the capacities of these ACs in DON adsorption. It can be seen that the carbon TY-202 presents maximum adsorption capacity for DON uptake. The capacity of the carbon GY-1 is lower than that of the carbon TY-202, while the carbon TY-1.5 presents the lowest capacity. The results indicate that the carbon prepared by peach is the most suitable type in adsorption of DON. From the results of the surface characterization shown in Table 1 and Fig. 1, though the carbon TY-8X30 and GY-1 present higher specific surface than TY-202 and TY-1.5, they possess lower capacities. It is reported that NOM is larger than most trace organic pollutants and the studies about the effect of pore size distribution on GAC adsorption of one type of NOM show that most of NOM are captured in pores with the size 3–10 nm [15,16]. Considering the DON solution was simulated by HA. It is possible that the adsorption capacities of these ACs depend on the amount of the mesopores. Therefore, ratios for the volume of meso and macropores to total pore volume are listed in Table 1. The results show that the ratio for samples GY-1 (0.41) and TY-202 (0.36) are much higher than TY-8X30 sample (0.21), revealing that the GY-1 and TY-202 samples have rich meso or marcoporous structures, which provide adequate pores available for molecule penetration. Therefore, the carbon GY-1 and TY-202 present higher capacity in DON adsorption. Although sample TY-1.5 has the highest ratio, they present the lowest adsorption capacity. The low capacity of TY-1.5 can be

Table 1
Properties of selected ACs

Model	Source	Type	BET surface (m^2/g)	Average pore size (nm)	Microporous volume, V_m (m^3/g)	Total pore volume, V_t (m^3/g)	$1\text{-}V_m/V_t$	pHpzc
GY-1	NPGC	Wood	837	2.138	0.265	0.447	0.407	6.7
TY-8X30	Wuxi Chi Kang Activated Carbon Co.	Coconut shell	917	1.936	0.349	0.444	0.214	6.9
TY-202		Peach	652	2.161	0.227	0.352	0.355	6.9
TY-1.5		Coal	714	2.039	0.215	0.364	0.409	5.4

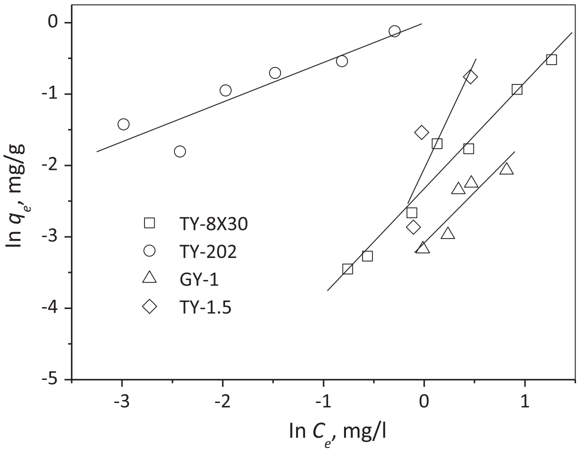

Fig. 2. Plots for Freundlich model for DON adsorption.

Table 2
Parameters of Freundlich model for DON adsorption by various ACs

Carbon types	K_f	1/n	R^2
TY-8X30	0.0978	1.490	0.97
TY-202	0.998	0.556	0.84
GY-1	0.046	1.422	0.82
TY-1.5	0.129	2.987	0.74

ascribed to its lower pH_{pzc} (point of zero charge, shown in Table 1). The lower pH_{PZC} of the sample means that the AC surface is negatively charged at neutral pH conditions. Due to the electrostatic repulsion between the negatively charged surface and the ionic species of DON [17], the capacity of the TY-1.5 in the adsorption of DON is likely to be reduced.

3.1.2. Adsorption kinetics

Kinetics studies were conducted to obtain useful data regarding the efficiency of adsorption and feasibility of scale-up operations. The experimental data show that most amounts of the DON are captured during the first 120 min of the adsorption, and the equilibrium tends to be established after approximately 240 min shaking. So, in practical application, 4 h is enough for the system of the DON adsorption to reach equilibrium. The pseudo-second-order model is applied to describe the kinetics of DON adsorption on AC. The equation of the pseudo-second-order model [18] is as follows:

$$\frac{dq_t}{dt} = k(q_e - q_t)^2 \tag{3}$$

where k (g/(min mg)) is the rate constant. q_t and q_e are the amounts of DON adsorbed at time t and the adsorption equilibrium. At initiation of the adsorption, $q_t = 0$. So the equation can be integrated to yield:

$$\frac{t}{q_t} = \frac{1}{kq_e^2} + \frac{t}{q_e} \tag{4}$$

The straight line plots of t/q_t against t under the conditions of different initial DON concentrations and adsorption temperatures can be tested to obtain the rate parameters shown in Fig. 3 (Fig. 3(a) for different initial DON concentration and Fig. 3(b) for different temperatures).

The parameters including k and q_e of the equation can be obtained from the intercept and slope of the plot of (t/q_t) vs. t. The results of the model fitting are present in Table 3. It can also be concluded from the table that with the increase of the initial DON concentration C_0 from 0.8 to 3.0 mg/l, q_e increases from 0.45 to 1.25 mg/g. The rate constant k_2 increases from 0.025 to 0.038 g/(min mg) with C_0 increasing from 0.8 to 1.0 mg/l. Further increase in the initial DON concentration C_0 brings a decrease in the rate constant to 0.007 g/(min mg). The increase in the reaction temperature from 283 to 323 K results in a decrease in the q_e from 1.38 to 0.94 mg/g. The high values of the coefficient R^2 shown in the table indicate that the process of DON adsorption by AC TY-202 can well be described by the pseudo-second-order model.

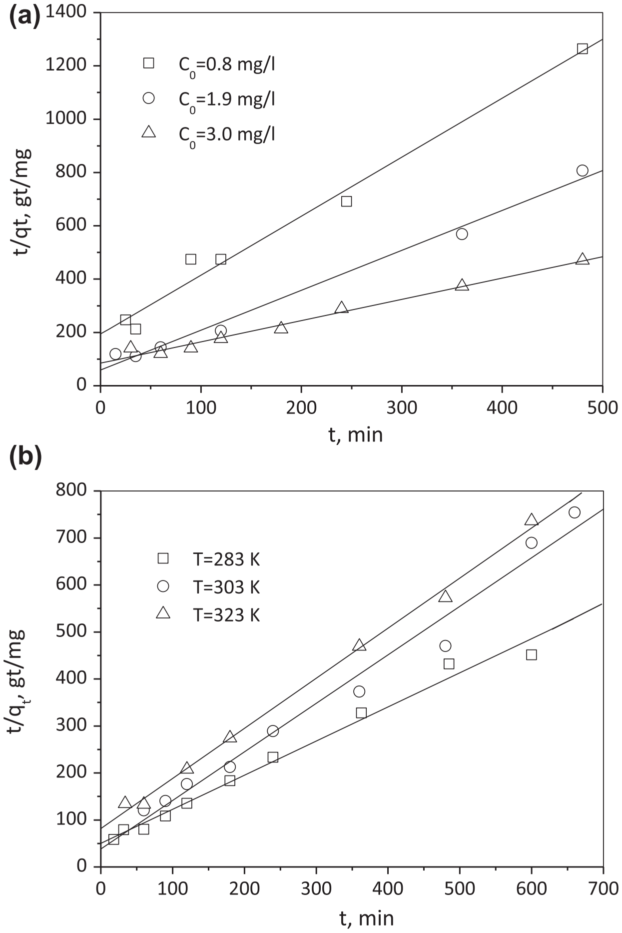

Fig. 3. Pseudo-second-order kinetic for the adsorption of DON on AC TY-202.

Thermodynamic behavior of DON adsorption by carbon was also investigated. Thermodynamic parameters including the changes in free energy (Δ*G*), enthalpy (Δ*H*), and entropy (Δ*S*) are obtained according to the experimental results and the following equations [19]:

$$\Delta G^0 = -RT \ln K_c \tag{5}$$

$$\ln K_c = -\frac{\Delta H^\circ}{R} \times \frac{1}{T} + \frac{\Delta S^\circ}{R} \tag{6}$$

where R is the ideal gas constant and K_c is the adsorption equilibrium constant. The values of enthalpy ΔH^0 and entropy ΔS^0 can be calculated from the slopes and intercepts of the plots of ln K_c vs. $1/T$ (shown in Fig. 4) by fitting the experimental data. Thermodynamic parameters obtained are given in Table 4. It is commonly reported that the absolute magnitude of the change in free energy for chemisorption is in a range of −80 to −400 kJ/mol, while physisorption is between −20 and 0 kJ/mol. The results obtained range from 4.8 to 9.6 kJ/mol, revealing that there is an energy barrier in the adsorption under the operation conditions, and the adsorption process is unspontaneous and less favorable at higher temperature [20].

The negative values of the standard enthalpy change (Δ*H*), which are −67.9 kJ/mol, indicates that the interaction between DON molecule and AC surface is exothermic in nature. In addition, the standard enthalpy change is higher than 40 kJ/mol, which indicates that the adsorption process is chemical in nature. These results confirm that the increase in the solution temperature would bring a decrease in DON adsorption. Furthermore, the negative value of Δ*S* supports the fact that the reaction is spontaneous at low temperature.

3.2. The adsorption in fixed bed columns

3.2.1. Effect of bed height

Accumulation of organic matters in the fixed-bed column is considered to be largely dependent on the quantity of sorbent contained in the column. So, different quantities of ACs are added into the column to produce different height of 3.5, 7.0, and 9.5 cm, respectively. The adsorption breakthrough curves obtained by varying the bed heights from 3.5 to 9.5 cm at 3.5 ml/min flow rate and 28.1 mg/L initial DON concentration are given in Fig. 5. It can be seen from the figure that both bed capacity and exhaustion time increase with bed height increase. It is commonly regarded that the mass transfer zone would be broadened and more binding sites can be available for adsorption with the increase in the bed height. Larger height provides greater adsorption sites and thus brings increases in bed capacity and exhaustion time [21]. The breakthrough time can be obtained directly from the

Table 3
Rate constants of the pseudo-second-order kinetic model

T, K	C_0, mg/l	Constants of pseudo-second-order kinetic model		
		q_e (mg/g)	k (g/(min·mg))	R^2
293	0.8	0.45	0.025	0.984
293	1.0	0.67	0.038	0.990
293	3.0	1.25	0.008	0.984
283	3.0	1.38	0.011	0.987
303	3.0	0.97	0.028	0.981
323	3.0	0.94	0.014	0.996

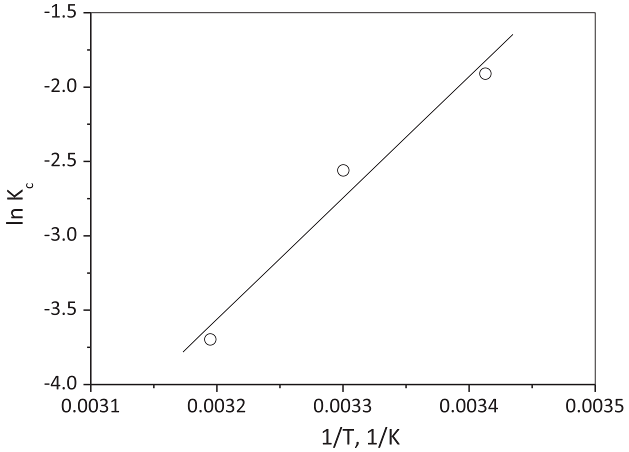

Fig. 4. Plot of ln K_C vs. $1/T$ for estimation of thermodynamic parameters.

Table 4
Thermodynamic parameters for the adsorption of DON

Temperature, K	ΔG, KJ/mol	ΔH, KJ/mol	ΔS, J/mol·K	R^2
293	4.81	−67.9	−246.8	0.970
303	6.66			
313	9.62			

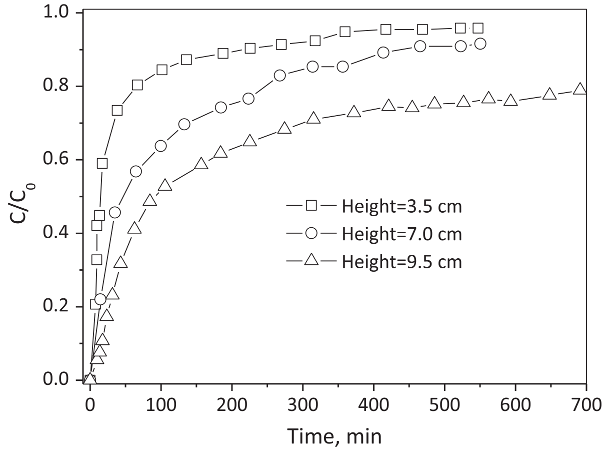

Fig. 5. Breakthrough curves for DON adsorption onto AC at different bed heights.

figure, and it increased from 1.41 to 6.44 min with the increase in the bed height from 3.5 to 7.0 cm. Further increase in the bed height to 9.5 cm brought further increase of the breakthrough time to 14.23 min. The capacity of AC increased with the increase in the bed height due to the fact that more binding sites were available for adsorption.

3.2.2. *Effect of flow rate*

Flow rate of the operation of the fixed bed is regarded as an important parameter affecting the adsorption of dissolved substances due to the transfer process. Therefore, in order to investigate the effect of flow rate on the adsorption of DON by AC particles packed in the column, flow rates from 1.1 to 3.5 ml/min are applied. Fig. 6 shows the variation of the normalized concentration of DON of the effluent with time for different flow rates. As indicated by the breakthrough curves, the breakthrough curve becomes steeper when the flow rate is increased.

The breakthrough time for the flow rate 3.5, 2.4, and 1.1 ml/min is 1.4, 5.1, and 21.2 min, respectively. It is obvious that the best performance appears at the flow rate of 1.1 ml/min. A higher flow rate decreases the external film mass resistance at the surface of the adsorbents because of the enhanced velocity shear, thus reducing the film thickness [21,22]. However, at the same moment, higher flow rate would lead to shorter breakthrough and exhaustion time. This is because that when the retention time of the solute in the column is not long enough for reaching equilibrium at that flow rate, the DON solution leaves the column before the equilibrium occurs. At higher flow rate, the contact time of DON with AC particles is very short, resulting in an earlier breakthrough and exhaustion time.

3.2.3. *Effect of initial DON concentrations*

The effect of influent DON concentrations on the breakthrough curves is shown in Fig. 7. It can be seen that the breakthrough time increases with the decrease

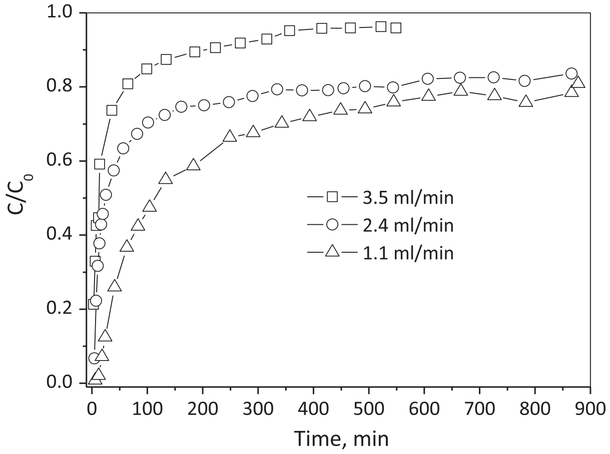

Fig. 6. Breakthrough curves for DON adsorption onto AC at different flow rate.

in the influent DON concentration. When the influent DON concentration decreased from 28.1 to 9.2 mg/l, the corresponding breakthrough time appears to increase from 1.4 to 2.8 min. At lower influent DON concentrations, since the lower concentration leads to a lower concentration gradient, the breakthrough comes slowly while the breakthrough curves were dispersed [22]. With the increase in the influent DON concentration, more adsorption sites are covered, thus bringing sharper breakthrough curves. These results show that the concentration gradient is one of the key parameters affecting the adsorption process.

3.3. Modeling of breakthrough curves

Adsorption in fixed bed column is a complex process and its performance is affected by many variables. The breakthrough time, exhaustion time, and effluent concentration is regarded as a practical important parameter to the design of the adsorption system. In this point of view, to facilitate the design of the adsorption column for DON removal, prediction of breakthrough curve in the proceeding of the adsorption in the column is desirable. Therefore, in this study, the adsorption data are fitted by using established models to determine the influence of different parameters for optimizing the fixed-bed adsorption process. Two models, namely Adams–Bohart and bed depth service time (BDST) models are applied.

3.3.1. Adams–Bohart model

The Adams–Bohart adsorption model is applied firstly. This model is commonly used in analyzing the initial stage of the breakthrough curve. It is assumed in the model that the rate of the adsorption is proportional to both the adsorbate concentration and the residual capacity of the adsorbent [23]. The model can be expressed as:

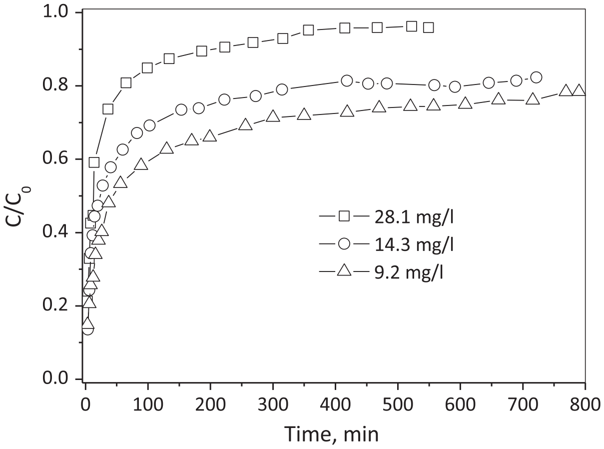

Fig. 7. Breakthrough curves for DON adsorption onto AC at different initial DON concentrations.

$$\frac{C}{C_0} = \exp\left(k_{\mathrm{AB}} C_0 t - k_{\mathrm{AB}} N_0 \frac{Z}{U_0}\right) \tag{7}$$

where N_0 is the maximum adsorption capacity (mg/g) and k_{AB} is the kinetic constant ($\mathrm{L\,mg^{-1}\,min^{-1}}$). Z is the height of the carbon bed and U_0 is the flow rate. After the fitting process, these characteristic parameters can be estimated. Table 5 shows the calculated values of N_0 and k_{AB}, as well as the correlation coefficients (R^2) for all breakthrough curves.

It can be seen from the table that the values of k_{AB} increase with the flow rate increase, while the increase in the initial DON concentration and bed depth bring a decrease of the values of k_{AB}. This shows that the overall system kinetics is dominated by external mass transfer in the initial part of adsorption in the column [24].

3.3.2. Bed-depth/service time analysis (BDST) model

BDST model is based on the assumption that the surface reaction between the adsorbate and the unused capacity of the adsorbent controls the adsorption rate. It is regarded as a simple model used in predicting the relationship between the service time, t and the packed-bed depth of the column, Z as well as other adsorption parameters. The BDST model [25] can be expressed as:

$$t_b = \frac{N_0}{C_0 F} Z - \frac{1}{K_a C_0} \ln\left(\frac{C_0}{C_b} - 1\right) \tag{8}$$

Table 5
Adams–Bohart parameters at different conditions

	Z, cm	C_0, mg/L	U_0, cm/min	$k_{\mathrm{AB}} \times 10^3$ L/mg min	N_0, mg/g	R^2
1	3.5	28.1	1.73	2.5	971.7	0.876
2	3.5	28.1	3.77	3.2	897.3	0.756
3	3.5	28.1	5.50	3.6	679.9	0.906
4	3.5	9.2	5.50	4.4	657.4	0.878
5	3.5	14.3	5.50	4.0	679.9	0.857
6	3.5	28.1	5.50	3.6	855.2	0.906
7	3.5	28.1	5.50	3.6	679.9	0.906
8	7.0	28.1	5.50	1.4	778.9	0.859
9	9.5	28.1	5.50	0.4	605.6	0.881

where C_0 is the influent concentration (mg/l), C_b is the effluent concentration (mg/l) at time t, K_a is the adsorption rate constant ($\mathrm{L\,min^{-1}\,mg^{-1}}$), N_0 is the adsorption capacity of the column (mg/l), Z is the bed depth of fixed-bed activated carbon (cm), F is the linear flow rate (cm/min), and t_b is the service time to breakthrough (min).

The BDST model shown above can be simplified into:

$$t_b = m_x Z - C_x \tag{9}$$

where

$$m_x = \frac{N_0}{C_0 F} \tag{10}$$

$$C_x = \frac{1}{K_a C_0} \ln\left(\frac{C_0}{C_b} - 1\right) \tag{11}$$

according to the equation above, the slope constant for different flow rates and influent concentrations can be directly calculated. The adsorption capacity (N_0) and the rate constant (K_a) can be obtained through the model. From the lines of t_b–Z at values of C_t/C_0 0.1 (shown in Fig. 8), the related constants are obtained. From the values of R^2 (0.94), the validity of the BDST model for the present system is confirmed. The BDST model constants can be applied in scaling up of the process for other conditions without further experimental runs.

The slope constant for a different flow rate can be directly calculated by following equation:

$$m'_x = m_x \frac{Q}{Q'} \tag{12}$$

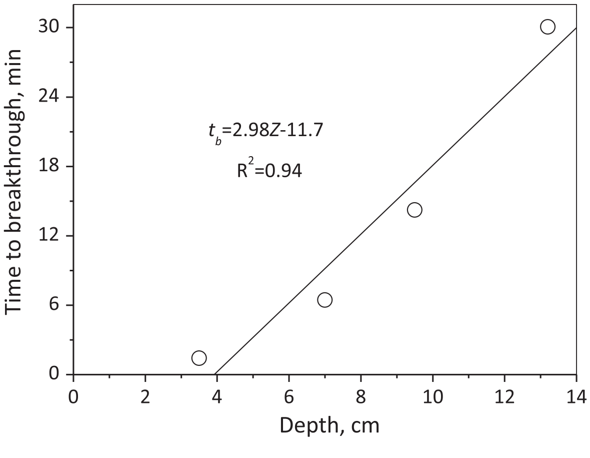

Fig. 8. Lines of t–Z at values of C_t/C_0 0.1.

Table 6
Predicted breakthrough time based on the BDST constants for new flow rates and influent concentrations

Q', ml/min	C_0', mg/l	Z, cm	m_x	m_x'	C_x, min	C_x', min	$t_{b^{theo}}$, min	$t_{b^{exp}}$, min
1.1	28.1	3.5	2.97	9.45	11.65	N/A	21.4	21.2
2.4	28.1			4.34			3.53	5.13
3.5	28.1			2.97			1.41	-1.24
3.5	9.20			9.12		22.8	9.17	9.25
3.5	14.3			5.85		18.5	2.00	2.77
3.5	28.1			2.97		11.7	1.41	-1.24

where m_x and Q are the old slope and influent flow rate, while m_x' and Q' are the new slope and influent linear velocity, respectively.

For other influent concentrations, the desired equation is given by the following expressions:

$$m'_x = m_x \frac{C_0}{C'_0} \tag{13}$$

$$C'_x = C_x \frac{C_0}{C'_0} \frac{\ln(\frac{C'_0}{C'_b} - 1)}{\ln(\frac{C_0}{C_b} - 1)} \tag{14}$$

where C_0' and C_0 are the new and old influent concentrations. C_x' and C_x are the new and old intercepts. C_b is the effluent concentration at influent concentration C_0 while C_b' is the effluent concentration at influent concentration C_0'.

Based on the constants obtained at a flow rate of 3.5 ml/min and influent concentration of 28.1 mg/l, performance of the adsorbent at other flow rates (1.1 ml/min and 2.4 ml/min) and influent concentration (9.20 mg/l and 14.3 mg/l) are predicted. The predicted time ($t_{b^{theo}}$) and experimental time ($t_{b^{exp}}$) are shown in Table 6. The differences between theory ($t_{b^{theo}}$) and experiment ($t_{b^{exp}}$) indicate that a good prediction has been gained for the case of changed flow rate and feed concentration at $C_t/C_0 = 0.1$. These results indicate that the equation can be applied to predict adsorption performance at other operation conditions for adsorption of DON onto AC particles.

5. Conclusion

On the basis of the experimental results, following conclusions can be drawn:

Peach carbon is suitable for DON adsorption than other selected activated carbons. It can be widely used in water treatment to remove DON from water.

Isotherm and kinetic studies are conducted. The isotherm data are described by the Freundlich model, while the kinetic data of adsorption are fitted by the pseudo-second-order kinetic model. Thermodynamic constants are also evaluated. The negative value of ΔS and ΔH reveals the exothermic nature and decrease in disorder of DON adsorption.

The performance of DON adsorption in fixed-bed column depends on the bed depth, flow rate, and influent DON concentration. As the flow rate or the influent concentrations increases, the breakthrough curve becomes steeper, while the break point time decreases.

Adams–Bohart model is applied to describe the initial region of breakthrough curve of DON adsorption under varying experimental conditions while the BDST model is applied to predict the breakthrough time for new flow rates and influent concentrations. Both models give good agreement with experimental curves.

Acknowledgments

The authors would like to acknowledge financial support for this work provided by the NSFC (No. 51208531 and 2011J05144).

References

[1] P. Westerhoff, H. Mash, Dissolved organic nitrogen in drinking water supplies: A review, J. Water Supply Res. 51 (2002) 415–448.

[2] W. Lee, P. Westerhoff, J.P. Croue, Dissolved organic nitrogen as a precursor for chloroform, dichloroacetonitrile, N-mitrosodimethylamine, and trichloronitromethane, Environ. Sci. Technol. 41 (2007) 5485–5490.

[3] W.H. Chu, N.Y. Gao, S.J. Zhao, H.P. Deng, The mechanism analysis of formation of chloroform during typical dissolved organic nitrogen tyrosine chlorination in drinking water, Acta Chim. Sinica 67 (2009) 2505–2510.

[4] L. Gu, B. Liu, X. Yu, Dissolved organic nitrogen (DON) in the processes of polluted source water treatment, Chinese Sci. Bull. 55 (2010) 3098–3101.

[5] R.M. Schneider, C.F. Cavalin, M.A.S.D. Barros, C.R.G. Tavares, Adsorption of chromium ions in activated carbon, Chem. Eng. J. 132 (2007) 355–362.

[6] A. Jusoh, L.S. Shiung, N. Ali, M.J.M.M. Noor, A simulation study of the removal efficiency of granular activated carbon on cadmium and lead, Desalination 206 (2007) 9–16.

[7] E.N. El Qada, S.J. Allen, G.M. Walker, Adsorption of basic dyes onto activated carbon using microcolumns, Ind. Eng. Chem. Res. 45 (2006) 6044–6049.

[8] J.W. Li, Z.B. Yu, M. Gao, X.P. Cai, Trihalomethanes adsorption on activated carbon fiber and granular activated carbon, Water Air Soil Pollut. 97 (1997) 367–378.

[9] J.M. Chern, Y.W. Chien, Adsorption of nitrophenol onto activated carbon: Isotherms and breakthrough curves, Water Res. 36 (2002) 647–655.

[10] A. Geethakarthi, B.R. Phanikumar, Adsorption of reactive dyes from aqueous solutions by tannery sludge developed activated carbon: Kinetic and equilibrium studies, Int. J. Environ. Sci. Technol. 8 (2011) 561–570.

[11] W. Chu, N. Gao, Y. Deng, M.R. Templeton, D. Yin, Impacts of drinking water pretreatments on the formation of nitrogenous disinfection by-products, Bioresour. Technol. 102 (2011) 11161–11166.

[12] SEPA, Water and Wastewater Monitoring Methods, Chinese Environmental 547, Science Publishing House, Beijing, 2002.

[13] Muhammad, T.G. Chuah, Y. Robiah, A.R. Suraya, T.S.Y. Choong, Single and binary adsorptions isotherms of Cd(II) and Zn(II) on palm kernel shell based activated carbon, Desalin. Water Treat. 29 (2011) 140–148.

[14] R.J. Qu, M.H. Wang, R.F. Song, C.M. Sun, Y. Zhang, X.Y. Sun, C.N. Ji, C.H. Wang, P. Yin, Adsorption kinetics and isotherms of Ag(I) and Hg(II) onto silica gel with functional groups of hydroxyl- or amino-terminated polyamines, J. Chem. Eng. Data 56 (2011) 1982–1990.

[15] K. Ebie, F. Li, T. Hagishita, Effect of pore size distribution of activated carbon on the adsorption of humic substances and trace organic compounds, Water Supply 13 (1995) 65–70.

[16] C. Pelekani, V.L. Snoeyink, Competitive adsorption in natural water: Role of activated carbon pore size, Water Res. 33 (1999) 1209–1219.

[17] X.J. Peng, Z.K. Luan, F.T. Chen, B.H. Tian, Z.P. Jia, Adsorption of humic acid onto pillared bentonite, Desalination 174 (2005) 135–143.

[18] L.C. Lei, X.J. Li, X.W. Zhang, Ammonium removal from aqueous solutions using microwave-treated natural Chinese zeolite, Sep. Purif. Technol. 58 (2008) 359–366.

[19] B.H. Hameed, A.A. Ahmad, N. Aziz, Isotherms, kinetics and thermodynamics of acid dye adsorption on activated palm ash, Chem. Eng. J. 133 (2007) 195–203.

[20] L.J. Kennedy, J.J. Vijaya, K. Kayalvizhi, G. Sekaran, Adsorption of phenol from aqueous solutions using mesoporous carbon prepared by two-stage process, Chem. Eng. J. 132 (2007) 279–287.

[21] G.M. Walker, L.R. Weatherley, Adsorption of acid dyes on to granular activated carbon in fixed beds, Water Res. 31 (1997) 2093–2101.

[22] L. Markovska, V. Meshko, V. Noveski, Adsorption of basic dyes in a fixed bed column, Korean J. Chem. Eng. 18 (2001) 190–195.

[23] S.H. Lin, R.S. Juang, Y.H. Wang, Adsorption of acid dye from water onto pristine and acid-activated clays in fixed beds, J. Hazard. Mater. 113 (2004) 195–200.

[24] R.P. Han, Y. Wang, X. Zhao, Y.F. Wang, F.L. Xie, J.M. Cheng, M.S. Tang, Adsorption of methylene blue by phoenix tree leaf powder in a fixed-bed column: Experiments and prediction of breakthrough curves, Desalination 245 (2009) 284–297.

[25] C.Y. Yin, M.K. Aroua, W.M.A.W. Daud, Fixed-bed adsorption of metal ions from aqueous solution on polyethyleneimine-impregnated palm shell activated carbon, Chem. Eng. J. 148 (2009) 8–14.